Perturbations of midlatitude subionospheric VLF signals associated with lower ionospheric disturbances during major geomagnetic storms

W. B. Peter,[1] M. W. Chevalier,[1] and U. S. Inan[1]

Received 1 August 2005; revised 30 November 2005; accepted 2 December 2005; published 10 March 2006.

[1] We examine the effects on the midlatitude ionospheric *D* region of the 7 April 2000 storm and the "Halloween storm" of late October 2003 by means of the associated perturbations of several subionospheric VLF signals propagating in both the northern and southern hemispheres. We use VLF nighttime data from the Holographic Array for Ionospheric/Lightning Research (HAIL), located in the United States ($L = 2-3$), as well as data from Palmer Station, Antarctica ($L = 2.4$). On 7 April 2000, a ~5 dB depression in VLF amplitudes is observed at multiple HAIL stations, with a depression onset that occurs later for VLF signal paths at lower latitudes. On both 7 April 2000 and 31 October 2003, fluctuations in the amplitude of the VLF signals are first observed in the premidnight sector and persist through the end of the data-recording period (dawn). The frequency content of the fluctuations is predominantly in the 0.01 to 0.02 Hz range but extends up to ~0.03 Hz. Increases in the energetic electron flux in the loss cone as measured by the NOAA-POES satellites are observed on both 7 April 2000 and 31 October 2003. We suggest that both the signal depressions and subsequent fluctuations are associated with variations in the precipitation flux of energetic electrons onto the upper atmosphere. Auroral activity patterns based on data from the NOAA-POES satellites show that the equatorward edge of the auroral oval expanded equatorward to lower *L* shells ($L < 3$) during both geomagnetic storms. Using the auoral activity patterns and multiple VLF/LF signal paths, we provide evidence that the fluctuations and the signal depression coincide with the equatorward edge of the auroral oval extending over the perturbed VLF/LF Great Circle Paths. Quantitative modeling of subionospheric VLF wave propagation incorporating energetic electron flux measurements (and the associated altitude profiles of secondary ionization) yields results consistent with the variations in the VLF signal amplitude observed.

Citation: Peter, W. B., M. W. Chevalier, and U. S. Inan (2006), Perturbations of midlatitude subionospheric VLF signals associated with lower ionospheric disturbances during major geomagnetic storms, *J. Geophys. Res.*, *111*, A03301, doi:10.1029/2005JA011346.

1. Introduction

[2] At the edge of the auroral zone, where the electrojet current system flows, high-energy ($E > 300$ keV) precipitating electrons cause local electron density enhancements in the ionosphere detectable through VLF remote sensing [*Kikuchi and Evans*, 1983]. The high-energy particle precipitation that usually accompanies the electrojet is a major source of energy input into the lower ionosphere [*Chenette et al.*, 1993]. Communication and navigation systems (e.g., VLF, LF, and GPS) can be significantly affected by ionospheric perturbations associated with the auroral electrojet and high-energy particle precipitation [*Inan et al.*, 1985; *Luo et al.*, 2002]. During periods of high geomagnetic activity, the effects of the auroral electrojet and the associated high-energy particle precipitation extend to midlatitudes, potentially causing severe problems with electric power delivery systems [*Ringlee*, 1989]. However, much of the focus of the impact of geomagnetic storms on the ionosphere has been at high latitudes [e.g., *Kikuchi and Evans*, 1983]. Ground-based VLF amplitude and phase measurements have previously been used as an indicator of the position of the auroral electrojet [*Cummer et al.*, 1996], albeit at higher latitudes than those considered here.

[3] Very low frequency (VLF) waves are guided within the spherical waveguide formed between the Earth and the ionosphere (Figure 1). The amplitude and phase of the subionospherically propagating VLF signals depend sensitively on the electrical conductivity of the lower ionosphere as well as that of the ground. The amplitude and phase of VLF transmitter signals observed at any point can thus be used to probe ionospheric processes that occur near ~85 km, the inferred nighttime upper reflection height of the waves. In this paper, we examine midlatitude ionospheric *D* region perturbations as detected by VLF signal variations associated

[1]Space Telecommunications and Radioscience Laboratory, Stanford University, Stanford, California, USA.

0148-0227/06/2005JA011346$09.00

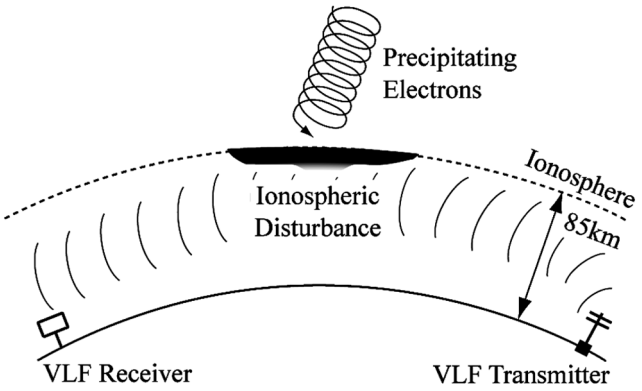

Figure 1. Cartoon depicting the earth-ionosphere waveguide, with a nighttime upper reflection height for VLF signals at ~85 km. Precipitating electrons produce secondary ionization, which in turn changes the electrical conductivity of the upper boundary of the Earth-ionosphere waveguide and perturbs the VLF wave propagating underneath.

with two geomagnetic storms, the 7 April 2000 storm and the "Halloween storm" of late October 2003.

[4] Figure 2 shows D_{st} and K_p indices for the two periods. For the 7 April 2000 storm, increased geomagnetic activity begins in the morning (Mountain Standard Time) of 7 April and persists through the night. For the Halloween storm, increased geomagnetic activity begins on the night of 29 October, with high levels of activity persisting through the night of 31 October. Moderate geomagnetic activity continued for several days afterward. The Halloween storm has a higher maximum K_p value than the 7 April 2000 storm, with peak activity occurring on both 29 and 31 October 2003.

[5] We examine the effects of these two geomagnetic storms on the midlatitude *D* region as measured by VLF signals. On 7 April 2000, a ~5 dB depression in VLF amplitudes was recorded at multiple HAIL stations, with a depression onset that occurred later for VLF signal paths at lower latitudes. On both 7 April 2000 and 31 October 2003, fluctuations in the amplitude of the VLF signals are first

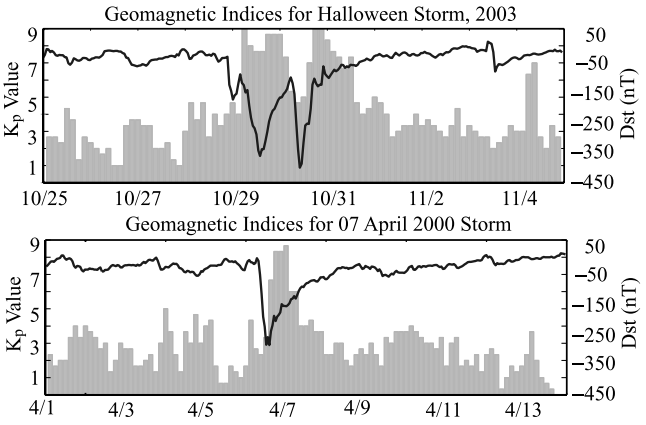

Figure 2. Geomagnetic indices. (a) Geomagnetic activity indices from 25 October 2003 to 5 November 2003. The D_{st} index is shown as a solid dark line, with the K_p index shown in light shading. (b) Geomagnetic activity indices from 1 April 2000 to 14 April 2000.

observed in the premidnight sector and persist through the end of the data-recording period (dawn). We suggest that both the signal depressions and subsequent fluctuations were associated with variations in the precipitation flux of energetic electrons onto the upper atmosphere and provide evidence that the fluctuations and the signal depression coincide with the equatorward edge of the auroral oval extending over the perturbed VLF/LF Great Circle Paths, consistent with the previous observations of *Cummer et al.* [1996]. The ability to locate and characterize the extension of auroral precipitation to lower latitudes should generate better understanding of the physical mechanisms linking geomagnetic activity and associated ionospheric disturbances.

1.1. Sources of Data

[6] We utilize subionospheric VLF signal data from the Holographic Array for Ionospheric/Lightning research (HAIL) and Palmer Station, Antarctica. Figure 3 shows the Great Circle Paths (GCPs) of subionospherically propagating VLF signals recorded at the HAIL array (top) and Palmer Station (bottom). The stations continuously monitor the amplitude and phase of coherent and subionospherically propagating VLF transmitter signals operated by the United States Navy in Washington (NLK at 24.8 kHz), Maine (NAA at 24.0 kHz), Hawaii (NPM at 21.4 kHz), and Puerto

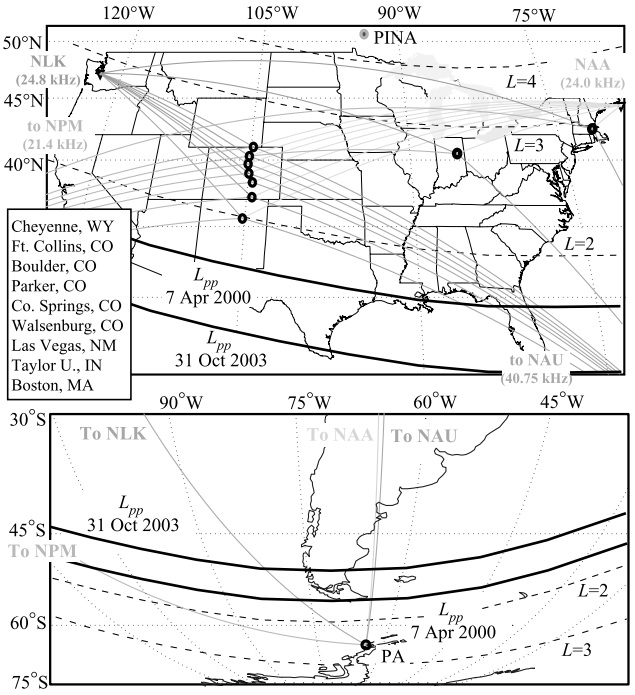

Figure 3. (top) Map of the Holographic Array for Ionospheric/Lightning research (HAIL). The Great Circle Paths (GCPs) of the subionospherically propagating VLF signals are shown as solid lines. The names of the receiver stations are shown in the box. Footprints of the $L = 2$ and $L = 3$ field lines are shown as dashed lines for reference. A solid black line denotes the plasmapause location (L_{pp}), projected down to 100 km altitude, for both 31 October 2003 and 7 April 2000. (bottom) Map showing Palmer station, Antarctica (PA). The GCPs of the VLF signals are shown as solid lines.

Rico (NAU at 40.75 kHz). Solid black lines denote the plasmapause projections (L_{pp}) for both 31 October 2003 and 7 April 2000. The 31 October 2003 plasmapause projection ($L_{pp} \sim 1.5$) was estimated from Extreme Ultraviolet (EUV) images from the IMAGE satellite published by *Baker et al.* [2004]. Owing to the absence of IMAGE satellite data for April 2000, the 7 April 2000 plasmapause projection ($L_{pp} \sim 1.7$) was estimated from the *Carpenter and Anderson* [1992] formula $L_{pp} = 5.6 - 0.46\ K_{p\max}$. On the basis of this formula, the plasmapause projection ($L_{pp} = 5.6 - 0.46 \times 9 \sim 1.5$) on 31 October 2003 is the same as that derived from the EUV IMAGE data. While the plasmapause projection is typically located poleward of both Palmer station and the HAIL receivers during quiet and moderate geomagnetic activity, the plasmapause projections on 31 October 2003 and 7 April 2000 were located at latitudes equatorward of both Palmer station and the HAIL array.

[7] The VLF data from the HAIL stations are typically acquired everyday from 0100 to 1300 UT, when the great circle paths (GCPs) between transmitter and receiver are partially or wholly in the nighttime sector. A $1.7 \times 1.7\ m^2$ magnetic loop antenna connected to a preamplifier is used to detect the VLF signal at all receivers. The broadband VLF signal is bandpass filtered to a range of 9–45 kHz and then is digitized at a rate of 100 kHz with 16-bit resolution, with triggers provided by GPS timing. Each receiver digitally down-converts the individual VLF transmitter signals and records the demodulated amplitude and phase with 20 ms resolution. The ''narrowband'' signal amplitude shown in many figures was measured with a 1000 tap, 200 Hz bandwidth filter around the transmitter frequency. At Palmer station, the receiving system consists of two orthogonal loop antennas, one facing north-south, the other east-west [*Wood and Inan*, 2002]. The detected broadband VLF signal is processed in the same fashion as the HAIL systems for narrowband acquisition.

[8] The VLF data presented in this paper is exclusively amplitude data (with the exception of Figure 10). Owing to the complicated modulation of the VLF transmitter signals, it is often difficult to accurately track the phase of the VLF signals for long periods (hours). Accordingly, continuous phase data was not available for significant periods on both 7 April 2000 and 31 October 2003. Long-term analysis of phase data is therefore difficult owing to gaps in the phase data. Furthermore, when the transmitter phase was properly tracked, the VLF phase signatures were not as clearly defined as in the amplitude data. Theoretically, phase data for single mode propagation of VLF signals has been shown to be more sensitive to ionospheric perturbations associated with high-energy precipitation [*Inan and Carpenter*, 1987]. It is not clear why the perturbations are not as well defined in the phase data, but such a result may be due to the multimode structure of the propagating VLF signal. Experimental measurements of multimode VLF signal perturbations associated with lightning [*Wolf and Inan*, 1990] showed that the magnitudes of simultaneous amplitude and phase events were only weakly correlated, often with different behaviors with time. The relative sensitivity of the amplitude and phase measurements was found to be highly dependent on the VLF path. However, the analysis of VLF phase data over short time periods provided additional information regarding the ionospheric perturbations (see Figure 10) for the cases considered in this work, and both amplitude and phase VLF measurements should be examined during geomagnetic disturbances. In this context, we note that a new algorithm for extracting the phase information continuously has now been added to the HAIL systems, to ensure the availability of both VLF phase and amplitude data in future studies.

2. Halloween Storm

[9] During the massive geomagnetic storm of late October 2003, the auroral oval extended down to midlatitudes. Figure 4 shows auroral activity patterns based on measurements from the NOAA-POES satellites' Total Energy Detector (TED) instruments, which monitor the power flux carried into the Earth's atmosphere by precipitating auroral charged particles with energies from 50 to 20,000 electron volts (eV). The images show that the auroral oval on the night of 26 October 2003 was located poleward of the HAIL and Palmer station GCPs. With the onset of the geomagnetic storm, the auroral oval extended equatorward to midlatitudes on both 29 October and 31 October 2003, with auroral precipitation at latitudes monitored by the HAIL and Palmer GCPs. By the night of 4 November 2003, the auroral oval had retreated poleward of the midlatitude HAIL and Palmer station paths.

2.1. VLF Perturbations

[10] The signal amplitude and phase of narrowband signals have long been used to detect disturbances in the VLF reflection height [e.g., *Cummer et al.*, 1997]. Figure 5 shows 4-hour panels of NLK amplitude data recorded at Palmer (PA) from 0300 to 0700 UT for each night from 27 October to 5 November. Figure 6 shows NLK amplitude data for the same times recorded at Walsenburg (WA). The ''narrowband'' data displayed here have a 200 Hz bandwidth centered on the NLK transmitter frequency of 24.8 kHz. Fluctuations in the signal are an indication of varying disturbances of the *D* region ionosphere along the GCP.

[11] During times of quiet geomagnetic conditions (26–29 October), the signal amplitude does not fluctuate significantly, indicating that the state of the *D* region (i.e., the altitude profile of secondary ionization) is relatively stable. Beginning on 30 October, fluctuations are evident, with the maximum activity occurring on the night of 31 October. It should be noted that while fluctuations in the VLF signal amplitude are recorded on 30 and 31 October 2003, there is no significant modulation on the night of 29 October 2003, despite high geomagnetic activity. The reason for this result is unclear. Magnetometer data from the CANOPUS array (PINA in Figure 3) and a USGS site in Boulder, Colorado both showed the onset of magnetic field perturbations at ~0630 UT on 29 October 2003. The onset of the magnetic field perturbations late in the night of 29 October suggests that the geomagnetic disturbance may not have significantly affected the *D* region midlatitude ionosphere until after the VLF acquisition period on 29 October. The increase in fluctuations on 31 October is observed on all the NLK and NAA signals received at the different HAIL stations, as well as several different signals received at Palmer. These fluctuations are therefore observed on both northern and southern hemisphere VLF signal paths. By 1–5 November,

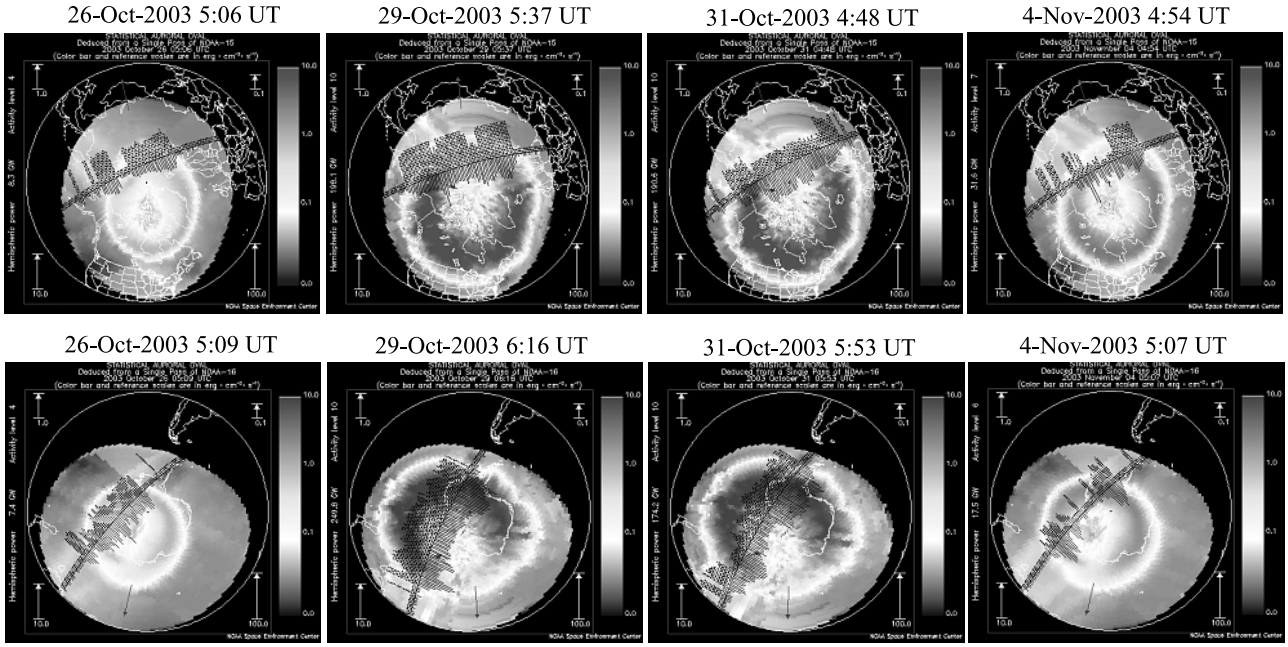

Figure 4. Auroral activity patterns for (from left to right): 26 October, 29 October, 31 October, and 4 November 2003. The top images are looking down on the northern Polar Cap, with the United States and the HAIL array located at the bottom of the images. The lower images are looking down on the southern Polar Cap, with Palmer Station and the southern tip of South America located at the top of the images. The auroral activity patterns are based on measurements from the NOAA-POES 15 and 16 satellites' Total Energy Detector (TED) instruments, which monitor the power flux carried into the Earth's atmosphere by precipitating auroral charged particles with energies from 50 to 20,000 electron volts (eV). The statistical patterns of auroral power flux are computed using observations obtained from more than 100,000 passes over both the northern and southern Polar Regions. The power fluxes in the statistical pattern are shaded on a scale from 0 to 10 ergs cm^{-2} s^{-1} according to the bars on the right. The satellite ground track (black line) and energy flux measurements (dashed black lines) used to create the statistical pattern of auroral precipitation are shown for each figure. The arrow points towards the noon meridian.

the signal amplitude has returned to its "quiet" conditions exhibited before the Halloween geomagnetic storm. In comparison with the auroral activity patterns (Figure 4), the fluctuations of the VLF signal amplitudes are enhanced on nights when the auroral oval had extended equatorward over the HAIL and Palmer station paths. This correlation supports the idea that the fluctuations are caused by variations in the auroral precipitation flux of energetic electrons that dominate the state of the *D* region during these disturbed times.

[12] In order to examine the frequency content of the fluctuations, we display the modulations of the VLF signal in the form of spectrograms (middle panels of Figures 5 and 6) produced by Fourier transformation of the time series of the narrowband amplitude data. The spectrograms of the narrowband NLK-PA amplitude data for 27 October, 31 October, and 5 November are shown in the middle panels of Figure 5. The spectrogram content represents amplitude modulation of the received NLK transmitter signal at Palmer. A pronounced increase in spectral content, extending up to ~0.03 Hz, was present from 0300 to 0900 UT (2100 to 0300 MLT) on 31 October. The middle panels of Figure 6 show similar spectral content in the modulations of the NLK-WA amplitude signal. The spectral content displayed in Figures 5 and 6 are typical of the fluctuations observed in NLK and NAA amplitude data recorded at the other HAIL receivers, as well as multiple VLF signals recorded at Palmer station.

[13] The onset of the fluctuations occurs in the premidnight sector (~0300 UT), with the fluctuations persisting throughout the night until dawn, when the sensitivity of the VLF signals to variations in the precipitation flux of energetic electrons diminished. The dramatic change in the VLF amplitude signal levels at 0900 UT is evidence of the day-night terminator moving across the path [*Uberall et al.*, 1982]. There is no evidence that the source of the fluctuations desists at dawn; rather the increased ionization levels typical of the dayside ionosphere likely dominate the mode propagation of VLF signals, making the VLF signals insensitive to fluctuations in precipitation flux on the scale observed during the nighttime.

[14] The bottom panels of Figures 5 and 6 show Fourier Transforms of the NLK-PA and NLK-WA amplitude signals for 27 October, 31 October, and 5 November. An increase in the frequency content of the fluctuations is evident on 31 October 2003. The modulations of the VLF contain the most structure in the 0.01 to 0.02 Hz range, corresponding to periodicities in the 50–100 s range. There is no indication of a single discrete frequency, which may indicate that the disturbances occurred at several discrete patches along or near the GCP, each with different and/or variable frequencies of modulation.

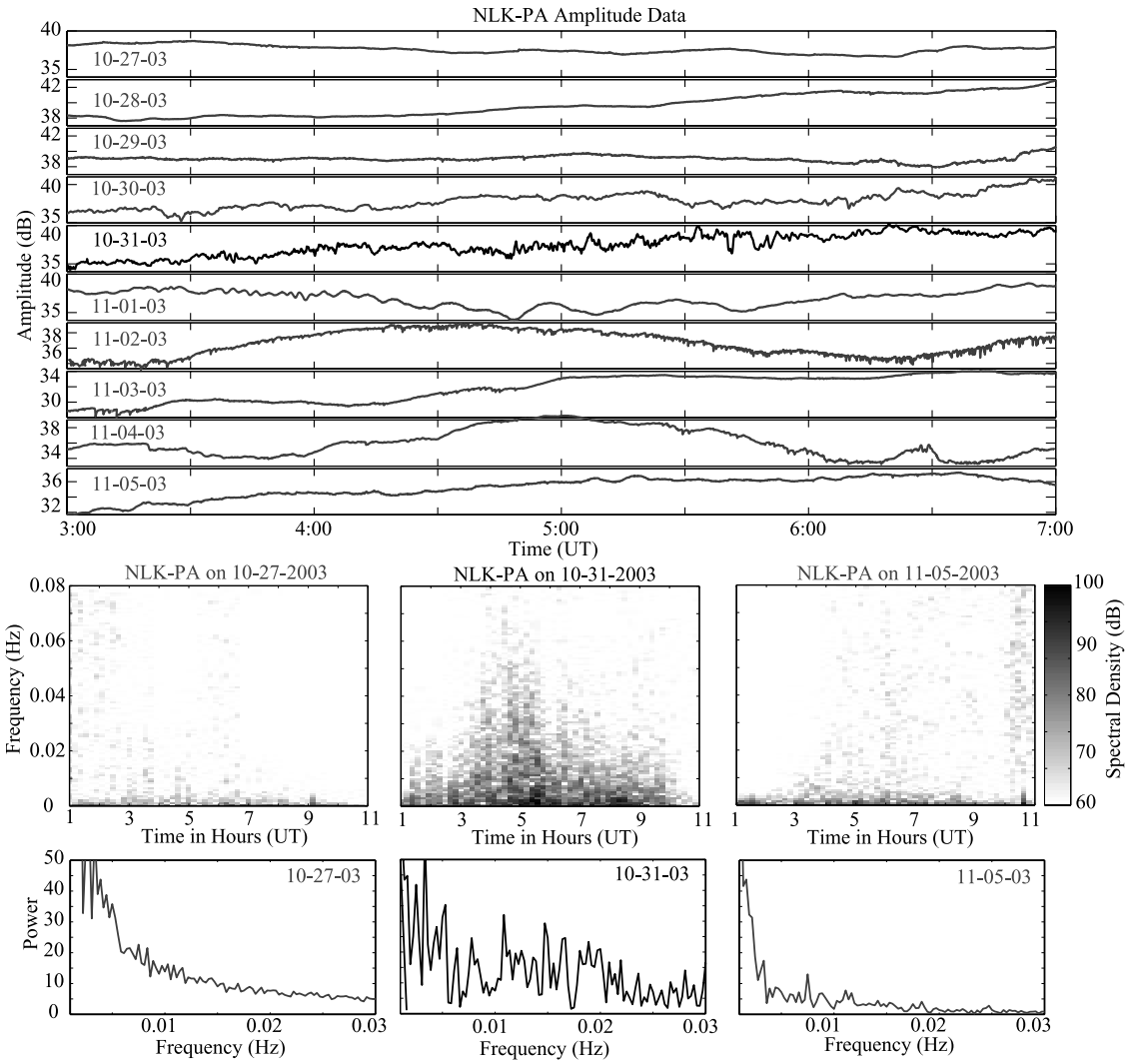

Figure 5. Halloween Storm VLF fluctuations in Southern Hemisphere. (top) Four-hour panels of the NLK amplitude data recorded at Palmer (PA) from 0300 to 0700 UT for each day from 27 October to 5 November. All panels show the signal amplitude on an 8-dB scale. (middle) Spectrograms of the narrowband NLK-PA amplitude signal for 27 October, 31 October, and 5 November. The spectral density intensity (as depicted by the shading) of each spectral component is plotted vertically as a function of frequency (modulation frequency of the VLF channels) and horizontally as a function of universal time. The spectrogram content represents amplitude modulation of the received NLK transmitter signal at Palmer. The spectrograms have a time resolution of ~20 min and a frequency resolution of ~0.76 mHz. A pronounced increase in spectral content, extending up to ~0.03 Hz, can be seen from 0300 to 0900 UT on 31 October. (bottom) Fourier Transform of the amplitude signal for the same three days, taken of data from 0300 to 0900 UT, giving a frequency resolution of $\sim 4.6 \times 10^{-5}$ Hz. An increase in frequency content is evident on 31 October 2003.

[15] In this context it is noteworthy that the chemical recovery times for secondary ionization in the nighttime *D* region are typically in the 10–100 s range [*Pasko and Inan*, 1994]. The recovery time is essentially the chemical response of the ionosphere to the newly introduced secondary ionization [*Pasko and Inan*, 1994] and is dependent on the conditions of the ionosphere and the energy spectrum of the precipitating electrons (which then determines the altitude at which the secondary ionization is produced). The energy spectrum of precipitation flux is determined to a large degree by the energy spectrum of the available trapped flux, known to be variable from day to day [*Demirkol et al.*, 1999; *Rees et al.*, 1988; *Gaines et al.*, 1995]. Bursts of precipitation (i.e., lightning-induced electron precipitation events) exhibit exponential recovery signatures [*Pasko and Inan*, 1994], which would result in a broad spectrum in the frequency domain. The recovery time of the ionosphere to precipitating electrons could effectively act as a filter and "smooth out" the frequency content of the VLF signal fluctuations (owing to the exponential recovery). While the time signatures of the fluctuations reported in this paper are not indicative of bursty precipitation events, the frequency content of the VLF signal fluctuations may be influenced by the recovery time of the *D* region ionosphere to the

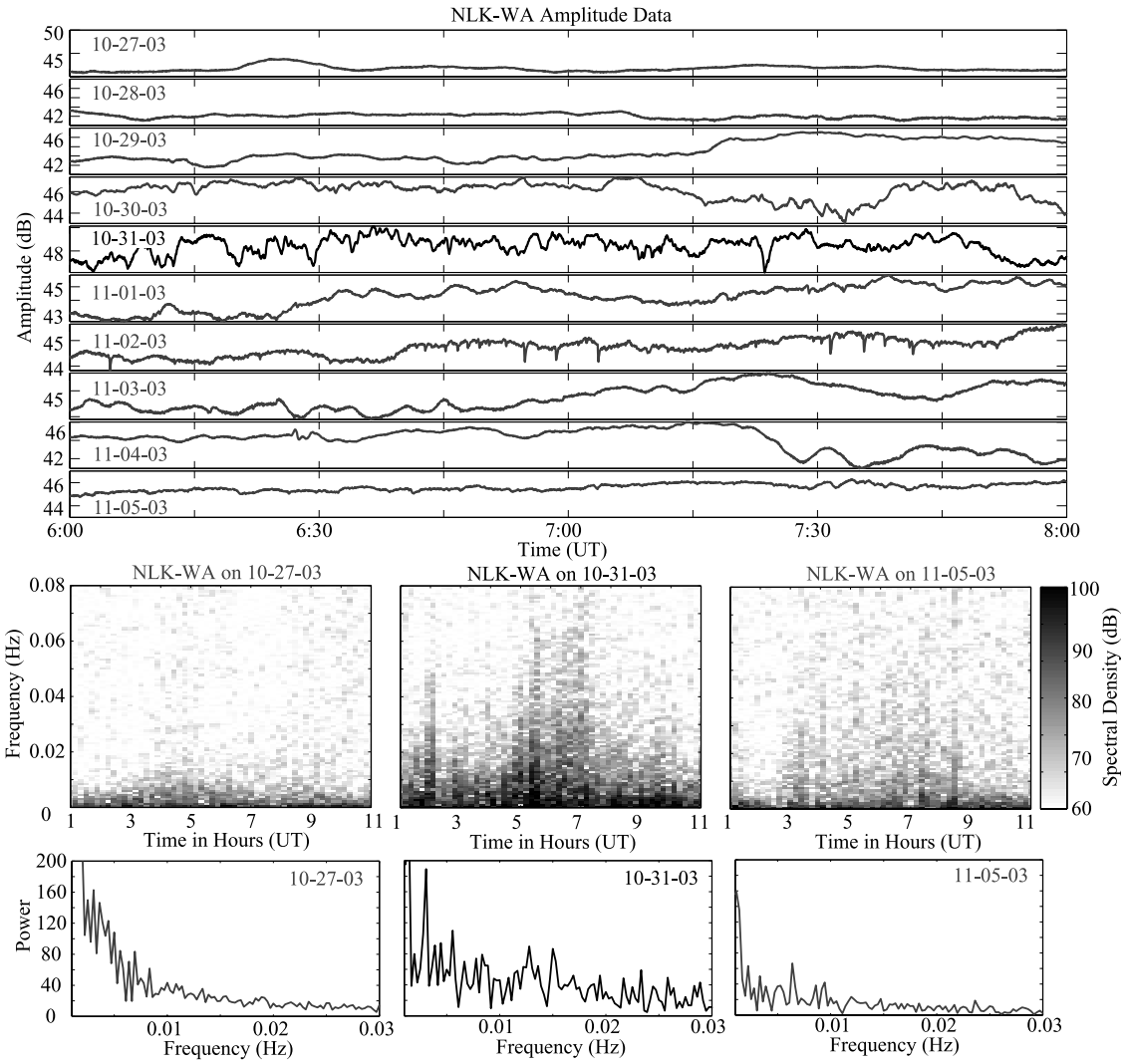

Figure 6. VLF fluctuations in Northern Hemisphere. (top) The same format as Figure 5, except the panels show NLK amplitude data recorded at Walsenburg, Colorado (WA). Fluctuations in the signal amplitude are evident on 31 October. (middle) Spectrograms of the narrowband NLK-WA amplitude signal for 27 October, 31 October, and 5 November. The spectrogram content represents amplitude modulation of the received NLK transmitter signal at Walsenburg. (bottom) Fourier Transform of the amplitude signal for the same 3 days, taken of data from 0300 to 0900 UT.

precipitation of energetic electrons. We assume, however, that the presence of structure in the frequency content of the VLF signal perturbations (from 0.01 to 0.02 Hz) is indicative of a modulated ionospheric disturbance.

2.2. Electron Precipitation

[16] In order to examine the influence of the Halloween storm on the precipitation flux of energetic electrons, we show in the top panel of Figure 7 data from the Medium Energy Proton and Electron Detector (MEPED) aboard the NOAA-16 POES satellite. The data shown is 16-s averaged 100–300 keV electron flux, energies typically associated with altering the reflection height of VLF signals via secondary ionization [*Lev-Tov et al.*, 1995]. For all passes, the detector remained nearly parallel to the magnetic field, typically within 10°. Furthermore, the variation of the angle with L shell was nearly identical (±2°) for each pass. The aperture of the detector has a 15° half-angle cone. Since the viewing angle (with respect to the magnetic field) of the detector is similar for each pass, the variations in flux observed for the different passes are not likely due to differences in the measurement angle. The bottom panel shows the tracks of the satellite passes with relation to the Palmer Station GCPs, projected down to 120 km altitude along the field line passing through the satellite. Data are shown for four passes, all of which occur between 0300 and 0900 UT, with each pass taking less than 10 min to cross over the region of interest. It is assumed that the data shown are representative of the flux of energetic electrons in the loss cone at the location of the Palmer Station GCPs.

[17] Prior to the geomagnetic storm (27 October), when the VLF signal amplitudes did not fluctuate significantly, the measured energetic electron flux levels were low. With the onset of geomagnetic activity, a sharp increase in the measured flux levels is observed across the L shells monitored by the HAIL and Palmer GCPs (L = 2–3). This increase

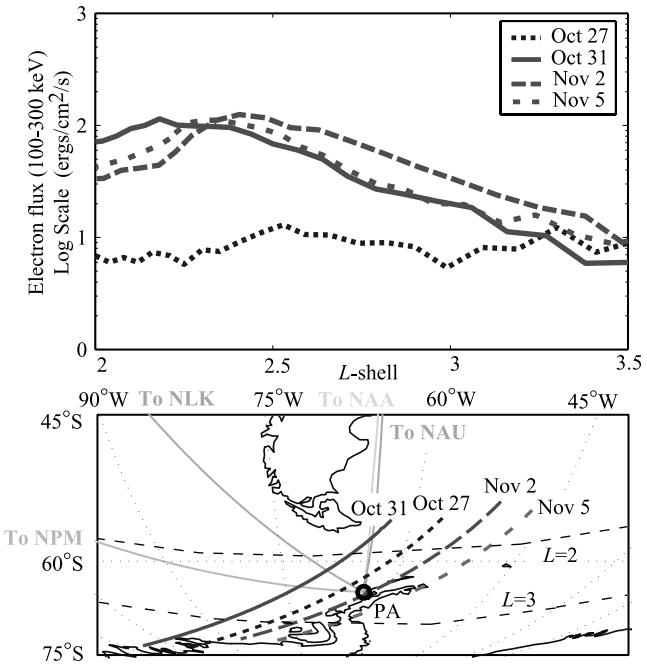

Figure 7. Flux levels in the loss cone. (top) Data from the Space Environment Monitor's (SEM-2) Medium Energy Proton and Electron Detector (MEPED) aboard the NOAA-16 POES satellite. The low altitude (830 to 870 km) polar-orbiting (98° inclination) satellite monitors the flux of energetic electrons. The data shown here is 16-s averaged 100–300 keV electron flux with the detector nearly parallel to the magnetic field. The data shown are assumed representative of the energetic electron precipitation flux as a function of L shell over the region. (bottom) A map shows the corresponding tracks of the satellite passes with relation to the Palmer Station GCPs, projected down to 120 km altitude along the field line passing through the satellite.

suggests that the energetic electron flux levels in the loss cone increased by at least an order of magnitude above levels typically observed during quiet geomagnetic conditions. It is during this time of increased loss cone flux (31 October) that the maximum activity in the VLF signal fluctuations is observed. The high levels of flux in the loss cone continue through 5 November but decrease from the 31 October levels for lower L shells ($2.0 < L < 2.2$). On the nights of 1–5 November, the VLF signal amplitude has returned to its "quiet" conditions exhibited before the Halloween geomagnetic storm. The presence of VLF signal fluctuations on 31 October but not on 1–5 November may be related to the different precipitation flux levels at lower L shells ($2.0 < L < 2.2$).

[18] It should be noted that variability in the background VLF noise recorded at Palmer station in the frequency range of the NLK transmitter can result in fluctuations in the amplitude of the narrowband NLK signal. To examine this possibility, broadband Palmer data on the night of 31 October was examined, with no quasi-periodic fluctuations in background noise visible. A 3-hour background narrowband signal was constructed from the Palmer broadband data with a center frequency of 27.0 kHz, close to that of the NLK transmitter (24.8 kHz) but not corrupted by the presence of any transmitter signals. This narrowband signal was taken with a 200 Hz bandwidth in the same manner the narrowband NLK-PK signal was generated, albeit at a higher center frequency. No quasi-periodic fluctuations were present in the background narrowband amplitude data. A Fourier transform of the constructed background narrowband signal also contained no significant frequency content. The absence of fluctuations in the constructed narrowband background data indicates that the fluctuations in the recorded NLK amplitude data are a result of modulation of the VLF transmitter signal, rather than variations in the background VLF noise at the location of the receiver. We therefore assume that the fluctuations observed on the VLF signals for both case studies (31 October 2003 and 7 April 2000) represent modulations of the amplitudes of the VLF transmitter signals.

3. The 7 April 2000 Geomagnetic Storm

[19] We now turn our attention to the 7 April 2000 geomagnetic storm, when geomagnetic activity increased on the morning of 7 April 2000 and persisted throughout the night (Figure 2). Figure 8 shows auroral activity patterns based on measurements from the NOAA-POES 15 satel-

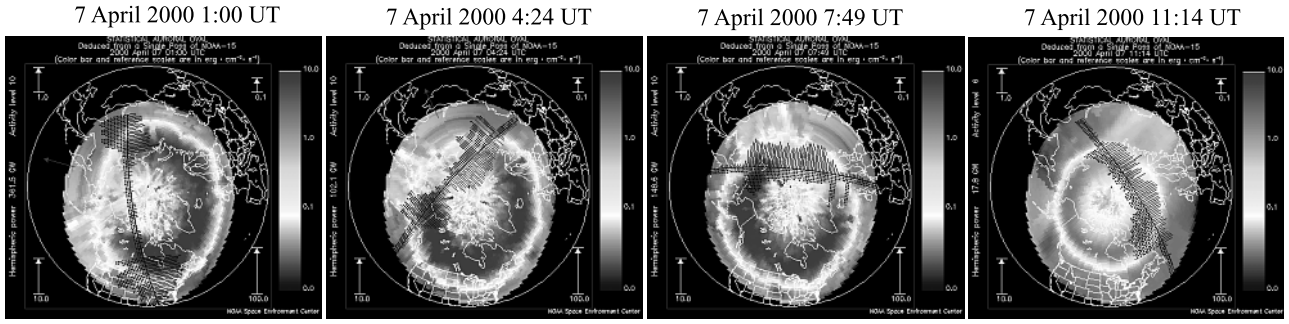

Figure 8. Auroral activity patterns for 7 April 2000 for (from left to right) 0100 UT, 0424 UT, 0749 UT, and 1114 UT. The auroral activity patterns are based on measurements from the NOAA-POES 15 satellite's Total Energy Detector (TED) instrument, which monitors the power flux carried into the Earth's atmosphere by precipitating auroral charged particles with energies from 50 to 20,000 electron volts (eV). All figures are of the same format as those in Figure 4. The auroral oval rotates through the HAIL paths over the course of the night.

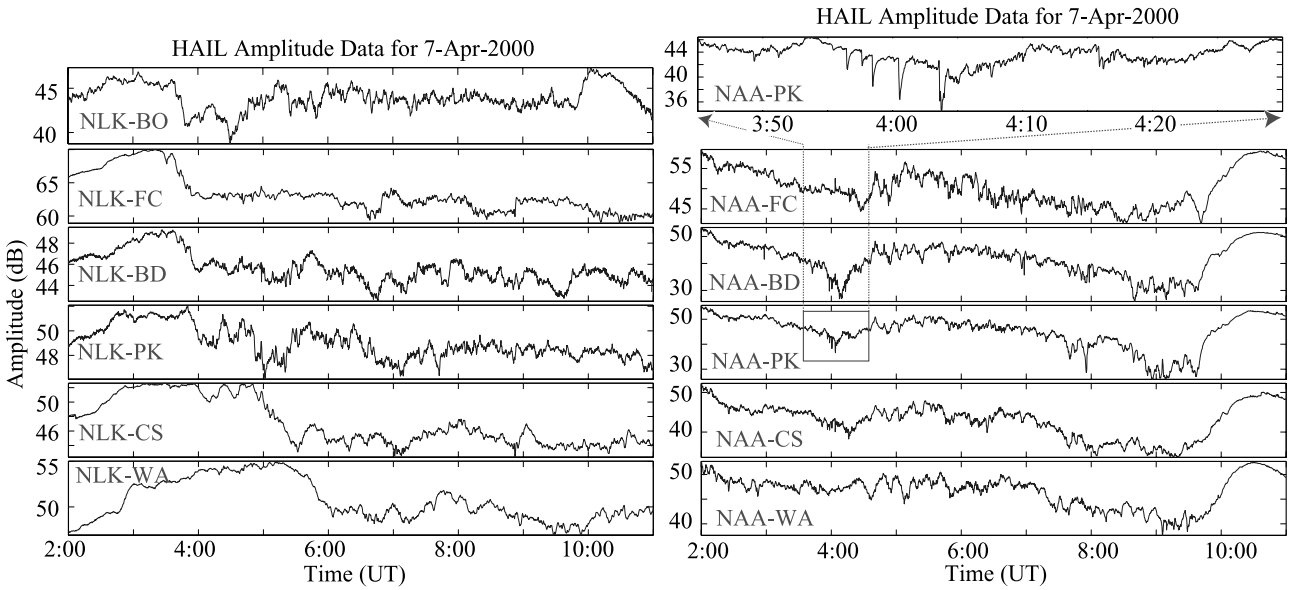

Figure 9. VLF Signal Amplitude on 7 April 2000. (left) Nine-hour panels of the NLK signal amplitude recorded at six HAIL VLF receivers. All panels show the signal amplitude on an 8-dB scale, with top to bottom corresponding to North to South GCPs. (right) Nine-hour panels of the NAA signal amplitude recorded at HAIL VLF receivers. The panels show the signal amplitude on different scales. A 45-min zoom-in of the NAA-PK signal shows the occurrence of several unusually large (>5 dB) LEP events.

lite's Total Energy Detector (TED) instrument of the same format as Figure 4. The images are for four times during the night of 7 April 2000 (0100, 0424, 0749, and 1114 UT), looking down upon the northern Polar Cap, with the United States and the HAIL array located at the bottom of the images. The images show that over the course of the night, the equatorially extended auroral oval rotates over the northern United States and through the HAIL GCPs. At 0100 UT, auroral precipitation is evident over both the northeastern U.S. and the GCPs between the NAA transmitter and the HAIL receivers. By 0424 UT, the auroral oval has rotated westward and overlays the GCPs between the NLK transmitter and the northern HAIL receivers. At 0749 UT, auroral precipitation is measured over most of the northwestern U.S., with the peak in auroral precipitation located at approximately the same longitude as the HAIL array. By 1114 UT, the auroral oval has retreated poleward of the U.S. with the decrease in geomagnetic activity.

3.1. VLF Perturbations

[20] Figure 9 shows 9-hour panels of NLK (left) and NAA (right) signal amplitude data recorded at six HAIL VLF receivers. The ''narrowband'' signal amplitudes shown in Figure 9 are of the same format as the data shown in Figures 5 and 6, with a 200 Hz bandwidth centered around 24.8 kHz (NLK) and 24.0 kHz (NAA). The NLK signal exhibits a ~4 dB decrease in amplitude, starting at ~0400 UT on the more northern paths (i.e., NLK-BO) and ~0530 UT on the southernmost path (NLK-WA). Following this depression, the NLK signal amplitude exhibits fluctuations similar to those observed on 31 October 2003 during the Halloween geomagnetic storm. The signal amplitude remains depressed throughout the night, until the day-night terminator moved across the GCPs at ~1100 UT. The onset of the signal depression roughly corresponds to the rotation of the auroral oval through the GCPs of the HAIL array (see Figure 8). The auroral oval likely overlies the more southern GCPs (i.e., NLK-WA) later as it rotates westward. By 0749 UT, all of the NLK GCPs are underneath the auroral oval, and all exhibit depressed signal levels with quasiperiodic fluctuations.

[21] Nine-hour panels of the NAA signal amplitude recorded at the HAIL receivers are shown on the right side of Figure 9. Fluctuations in the amplitude of the signal are evident at the beginning of the data acquisition (0100 UT) and persist through 0900 UT when the day-night terminator moved over the eastern GCPs. As the NAA transmitter is located in the northeastern United States, the auroral oval already overlies the NAA GCPs at the start of the data acquisition (0100 UT). The occurrence of auroral precipitation throughout the night over the NAA GCPs coincides with the presence of fluctuations in signal amplitude throughout the night. The top right panel is a 45-min zoom-in of the NAA-PK signal, showing the occurrence of several unusually large (>5 dB) perturbations known as Lightning-Induced Electron Precipitation (LEP) events, possibly indicating an increase in trapped energetic electron (100–300 keV) flux levels in the radiation belts [*Peter and Inan*, 2004].

[22] The top panel of Figure 10 shows NAA signal phase data recorded at the HAIL receiver sites from 0415 to 0600 UT on 7 April 2000. A rapid increase in phase over the course of a few minutes, starting at ~0500 UT, is evident on all of the signals. The bottom panel shows a 10-min zoom-in of the NAA signal phase for each of the sites. Phase data recorded at sites of higher latitude exhibit an earlier onset and increased total phase change than data recorded at lower-latitude sites. The NAA-PK data exhibit a phase change of ~200 degrees over the course of 4 min, or a change of ~0.83 degrees per second. Phase changes of this

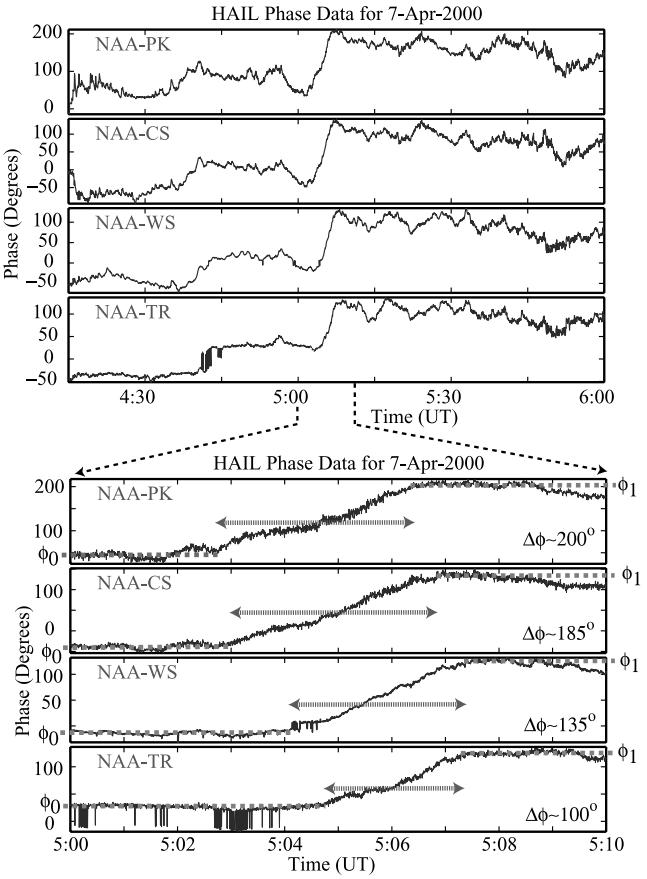

Figure 10. VLF Signal Phase on 7 April 2000. (top) Panels of the NAA signal phase from 0415 to 0600 UT recorded at four HAIL sites, with an increase in phase starting at ~0500 UT. (bottom) A zoom-in of the NAA signal phase showing an earlier onset and increased total phase change for higher latitude GCPs. The symbol ϕ_0 denotes the ambient phase prior to the increase in phase, with the symbol ϕ_1 denoting the phase after the increase. The green line denotes the time over which the phase change occurs, with the total phase change ($\Delta\phi$) shown on the right of each panel.

scale are highly atypical for the nighttime signals recorded by the HAIL array. The timescales of the phase change (on the order of a few minutes), precludes the possibility that the change was due to the rotation of the auroral precipitation over the paths. Instead, this rapid phase change may have been correlated with a rapid expansion of the auroral electrojet equatorward [*Kikuchi and Evans*, 1983; *Cummer et al.*, 1996].

[23] Neither the NLK signal amplitude depression nor the subsequent fluctuations observed on 7 April 2000 are typically observed on the HAIL array during quiet or moderate geomagnetic conditions. NLK signal amplitude data for six different HAIL stations is shown in Figure 11 for 6 April (left) and 7 April (right). The data for 7 April are identical to those shown in Figure 9. The depression in signal amplitude and subsequent fluctuations exhibited on 7 April are not evident on 6 April. The bottom panels of Figure 11 show two spectrograms of the NLK-PK signal for 6 April (left) and 7 April (right), of a format similar to the spectrograms shown in Figures 5 and 6. The 7 April spectrogram shows increased frequency content after 0400 UT, roughly the same time as the onset of fluctuations in the NLK-PK signal amplitude. The NLK-PK spectrogram on 7 April 2000 is similar to the spectrograms of the NLK signal amplitudes recorded at Walsenburg and Palmer on 31 October 2003 during the "Halloween storm." The frequency content extends up to ~0.03 Hz, with no indication of a single discrete frequency component. The onset of fluctuations in the NLK-PK amplitude data occur immediately after the depression of the signal amplitude, suggesting that the signal depression and subsequent fluctuations are due to the same source mechanism.

3.2. LWPC Model Calculation

[24] In order to estimate the significance of the amplitude depression and subsequent fluctuations in terms of electron precipitation, we use a quantitative model of the VLF subionospheric wave propagation together with precipitation flux measurements from four satellite passes. The left-hand panels of Figure 12 show electron flux measurements from the NOAA-16 POES satellite, of the same format as Figure 7, with the detector oriented nearly parallel to the magnetic field. The data shown is assumed to be representative of the precipitation flux at 30–100 keV (top), 100–300 keV (middle), and 300–1100 keV (bottom) as a function of L shell over the region. Data from four satellite passes are shown. The first (A) occurs at 0254 UT on 6 April, prior to the onset of geomagnetic activity. The second (B) occurs at 0437 UT, also before the onset of geomagnetic activity and with similar flux profiles at each of the three energy ranges to those measured at time A. The third pass (C) occurs after the advent of geomagnetic activity, at 0237 UT on 7 April 2000. A sharp increase in precipitation flux is observed on all three channels. Note the variations in flux levels with L shell, especially the peak in flux between $L = 2.5$ and $L = 2.7$ (particularly evident on the 100–300 keV channel). The fourth pass (D) occurs shortly after the third pass, at 0414 on 7 April. The elevated flux levels are still observed, although the peak in flux between $L = 2.5$ and $L = 2.7$ is no longer observed.

[25] Note that the third satellite pass (C) occurs prior to the depression of the NLK signals (which occurred at ~0400 UT) in the HAIL data, yet we assume that the flux profiles recorded during satellite pass C were characteristic of the precipitation flux at the NLK GCPs on the night of 7 April 2000 that resulted in the signal depression in amplitude as labeled (C) in Figure 11. It is important to note that we do not assume the satellite observations to be exact measurements of the precipitation fluxes that occurred over the GCPs. Instead, the model calculation uses the measured flux profiles to ascertain whether the disturbances in the VLF amplitude data are consistent with possible flux profiles that occurred during these times and to gain an idea of the sensitivity of VLF signal amplitude to changes in the precipitation flux.

[26] We use the four different flux profiles as recorded by the NOAA-POES satellite to generate ionospheric electron density profiles as a function of L shell. The L range is sampled using 10 equidistant great circle segments along magnetic latitude as illustrated by the line segment with alternating shadings denoted with asterisks in Figure 12.

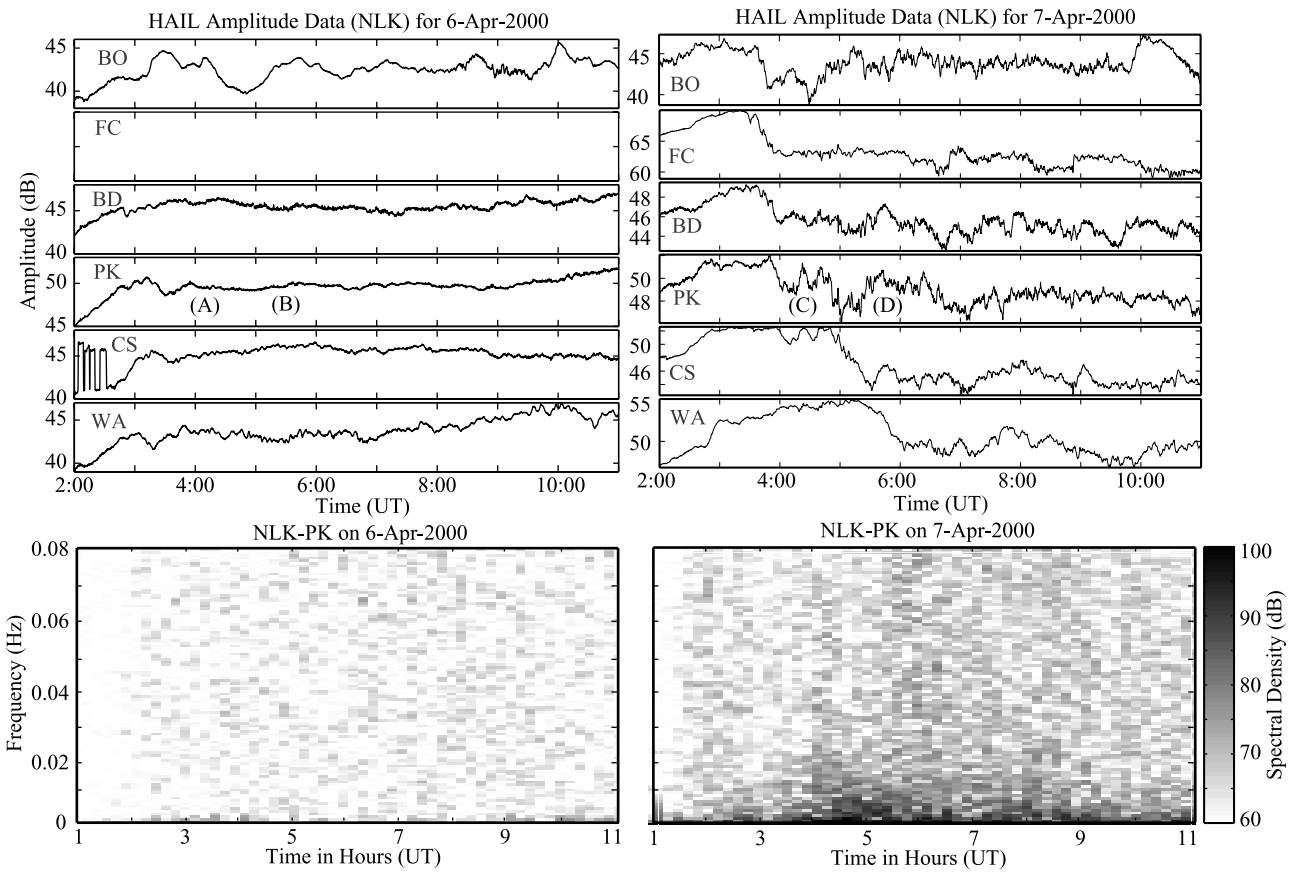

Figure 11. NLK Amplitude Data on 6 April and 7 April 2000. (top) Nine-hour panels of the NLK signal amplitude recorded at six HAIL VLF receivers on 6 April (left) and 7 April (right). All panels show the signal amplitude on an 8-dB scale, in the same format as Figure 9. Data for NLK-FC on 6 April are missing due to equipment malfunction. The letters (A), (B), (C), (D) denote the signal amplitudes that were compared to LWPC model calculations (see Figure 12). (bottom) Spectrograms of the narrowband NLK-PK amplitude signal for 6 April (left) and 7 April (right) from 0100 to 1100 UT. The figures are of the same format as the spectrograms of Figures 5 and 6. The spectrogram content represents amplitude modulation of the received NLK transmitter signal at Parker. An increase in the frequency content of the fluctuations was evident on 7 April 2000.

The fluxes from the satellites are then averaged over each segment and used as inputs into a Monte-Carlo simulation of the penetration of energetic electrons into the ionosphere to determine the amount of secondary ionization produced by energetic electron precipitation as a function of altitude [*Lehtinen et al.*, 2001]. The secondary ionization rates, as well as the ambient ionization rate (i.e., the ionization rate without precipitation), are used in an ionospheric chemistry model [*Glukhov et al.*, 1992; *Pasko and Inan*, 1994] to obtain electron density profiles for each of the ten segments. These ionospheric electron density profiles are then mapped to ten segments along the NLK-PK GCP (denoted as alternate shadings along the GCP in Figure 12), assuming the electron density varied only in *L* shell. Finally, for each of the four satellite passes, the NLK signal propagation and resultant amplitude measurements at a HAIL site located in Parker, Colorado were determined using the Long Wave Propagation Capability (LWPC) code [*Feguson and Snyder*, 1987; *Poulsen et al.*, 1993] with the ten segments of previously calculated ionospheric electron density profiles along the NLK-PK GCP as input.

[27] The results of the model calculations are shown in the bottom right panel of Figure 12. Using precipitation flux data from satellite pass A, the calculated NLK-PK amplitude is assumed representative of ''quiet'' geomagnetic conditions. The model calculations yield similar amplitudes for passes A and B, with a difference of less than 0.5 dB. The similar results for cases A and B are consistent with the NLK-PK amplitude data on 6 April, which varies little over the course of the night. Calculations for pass C yield a signal amplitude level significantly depressed ($\sim$5 dB) in comparison with those of passes A and B. This result indicates that the changes in precipitation flux measured by the NOAA-POES satellite between pass C and passes A and B could have resulted in the depression of the NLK signal amplitude observed on 7 April 2000 (at $\sim$0400 UT). There is a difference of $\sim$1 dB in the NLK-PK amplitude between calculations using passes C and D, which is consistent with the scale of the fluctuations observed on the NLK-PK signal subsequent to the signal depression. In summary, the LWPC model calculations incorporating NOAA-POES satellite measurements yield results consis-

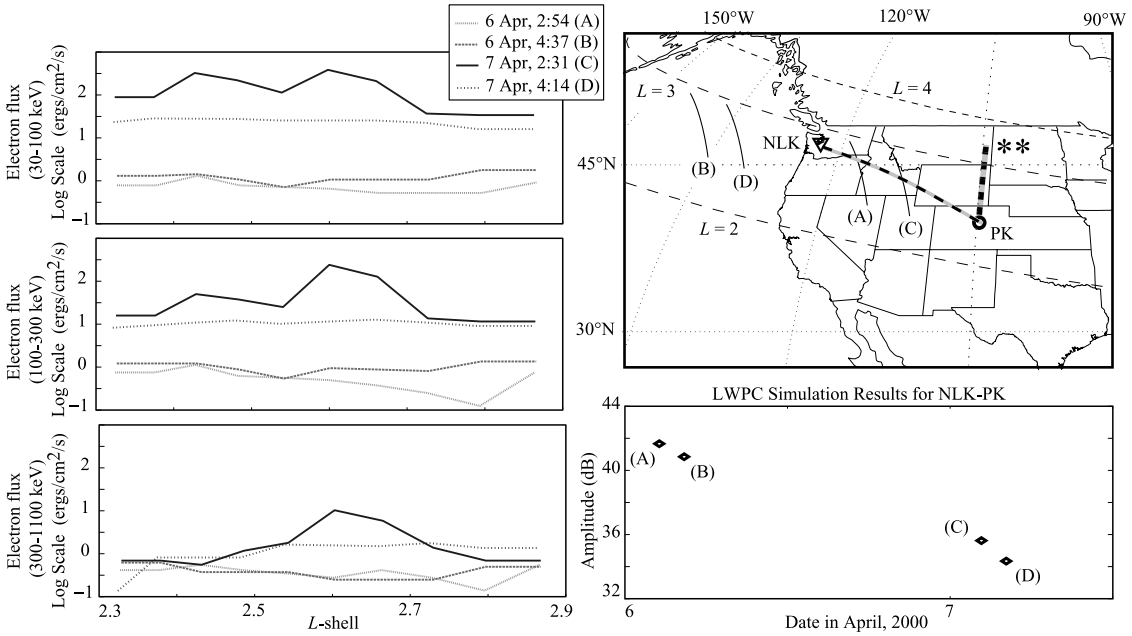

Figure 12. Model calculations for the 7 April 2000 storm. (left) Data from the NOAA-16 POES satellite, of the same format as Figure 7. The data shown is 16-s averaged 30–100 keV (top), 100–300 keV (middle), and 300–1100 keV (bottom) electron flux with the detector nearly parallel to the magnetic field. The satellite passes occurred between 0200 and 0500 UT, with two passes (A and B) occurring on 6 April and two more (C and D) occurring on 7 April. (top right) A map shows the corresponding tracks of the satellite passes with relation to the NLK-PK GCP, projected down to 120 km altitude along the field line passing through the satellite. The *L* range of the NLK-PK GCP is sampled using ten equidistant great circle segments along magnetic latitude as illustrated by the line segment with alternating shadings denoted with asterisks. The ten segments of ionospheric density profiles along the NLK-PK GCP used in the modeling are also denoted with alternating shading. (bottom right) Results of the LWPC model calculation of the NLK-PK subionospherically propagating signal amplitude. The black diamonds represent the relative magnitude of the NLK-PK amplitude generated by the model using precipitation flux data from the four satellite passes.

tent with the variations in the amplitude of the NLK-PK signal observed on 6 and 7 April 2000.

4. Discussion

[28] The depression and variation of the NLK-PK signal amplitude are shown to be consistent with measured variations in the energetic electron precipitation flux as recorded by the NOAA-POES satellite. The satellite recorded variations in precipitation flux extending up to energies greater than 1 MeV. The largest increase is in the energy range 100–300 keV, those energies thought to be most effective in altering the *D* region conductivity [*Demirkol et al.*, 1999]. VLF propagation model calculations performed by *Cummer et al.* [1997] showed that observed VLF amplitude decreases were consistent with propagation under conditions of enhanced *D* region ionosphere electron densities caused by auroral electron precipitation. The *Cummer et al.* [1997] paper also suggested that electrons with energies greater than 100 keV were responsible for the VLF amplitude depressions observed. Variations in electron precipitation flux with energies greater than 100 keV could explain the behavior of the VLF signals observed during the two storms considered. Future studies of VLF signal fluctuations during geomagnetic storms are needed to more conclusively determine the sources of variations in precipitation flux.

4.1. Possible Sources of Signal Perturbations

[29] The enhanced flux in the loss cone of 100–300 keV electrons may indicate enhanced radiation belt loss processes induced by wave-particle interaction. Accordingly, ground-based Palmer broadband VLF recordings were examined for the night of 31 October 2003. No indication was found of enhanced chorus or midlatitude hiss activity on the night of 31 October, and the recorded spectral content from 1 to 5 kHz was actually depressed on 31 October in comparison with the nights before and after 31 October. While we only examined ground based measurements of chorus and hiss activity, the ''quiet'' conditions of 31 October as recorded at Palmer suggest that the increased precipitation observed on the NOAA-POES satellite may not have been due to increased natural wave activity in the magnetosphere.

[30] A possible source of the modulation in precipitation flux is ULF geomagnetic pulsations. In a study of amplitude modulations of ELF/VLF (0.5–4.0 kHz) radio wave power recorded at the South Pole [*Smith et al.*, 1998], daytime quasi-periodic fluctuations consisted of a broad modulation

band centered at ~30 mHz. The quasi-periodic events were attributed to field line resonance modulating the whistler mode wave growth rates in the high-altitude VLF/ELF source region. In order to examine the possible role of ULF waves and magnetic field fluctuations in the VLF perturbations, magnetometer data was examined for both storm periods. Magnetic field measurements for 7 April 2000 from the southernmost magnetometer (PINA) in the CANOPUS array are shown in Figure 13a. The location of the magnetometer is shown in Figure 3. The magnetometer data for the night of 7 April shows the onset of magnetic field fluctuations at ~0430 UT. The magnetic field, as measured by the PINA magnetometer, exhibited fluctuations similar in timing and frequency content (Figure 13b) to the perturbations in the NLK and NAA signal amplitudes (see Figure 9). Similar fluctuations in magnetic field strength were also observed on 31 October 2003. Magnetometer measurements are frequently used to detect the onset of geomagnetic substorms through the presence of geomagnetic bays and Pi 2 ULF waves [*Kikuchi and Evans*, 1983; *Smith et al.*, 2002]. The presence of magnetic field fluctuations suggests a possible link between ULF waves and the precipitation modulation (by ULF modulation of VLF growth rates in the equatorial plane or more direct effects). However, it is inconclusive without further study whether field line resonances and/or ULF geomagnetic pulsations played a role in the fluctuations observed during the two storms examined in this study.

[31] During geomagnetic disturbances, particle populations characteristic of the auroral region expand equatorward and their effects are felt at previously subauroral latitudes [*Foster et al.*, 1998]. The increase in the loss cone flux of electrons with energies greater than 100 keV for 7 April 2000 and 31 October 2003 indicates that the energy spectrum of the precipitation was more energetic than that typically associated with auroral precipitation [*McEwen et al.*, 1981; *Ostgaard et al.*, 2001]. Examination of riometer data from PINA on 7 April 2000 (Figure 13c) suggests an onset of enhanced absorption at ~0430 UT, with a continued increase in absorption through ~0800 UT. The absorption, as measured by the PINA riometer, exhibited fluctuations similar in timing and frequency content to the perturbations in the NLK and NAA signal amplitudes (see Figure 9). Enhanced absorption is frequently used as an indication of energetic electron (>10 keV) precipitation [*Stauning*, 1997], and while the PINA riometer is located north of the HAIL array, this result supports the hypothesis that energetic electron precipitation is responsible for the VLF perturbations observed.

[32] VLF remote sensing has previously been used to detect the expansion of high-energy auroral particle precipitation to midlatitudes. *Cummer et al.* [1997] compared nighttime observations of the amplitude of the NLK transmitter signal as recorded in Gander, Newfoundland with UARS satellite measurements of auroral precipitation during November 1993 and January 1994. Almost 94% of the particle precipitation onsets recorded by the satellite during those 2 months could be readily identified in the VLF amplitude data. *Foster et al.* [1998] examined the 3–4 November 1993 geomagnetic storm using amplitude perturbations of VLF signals to localize the energetic electron precipitation to between 56 and 58.5 degrees latitude and resolved the precipitation onset to the premidnight sector. *Cummer et al.* [1996] associated ground-based VLF amplitude and phase perturbations with movements of the auroral electrojet and associated high-energy precipitating electrons. The previous studies [*Kikuchi and Evans*, 1983; *Cummer et al.*, 1996] neither reported nor considered

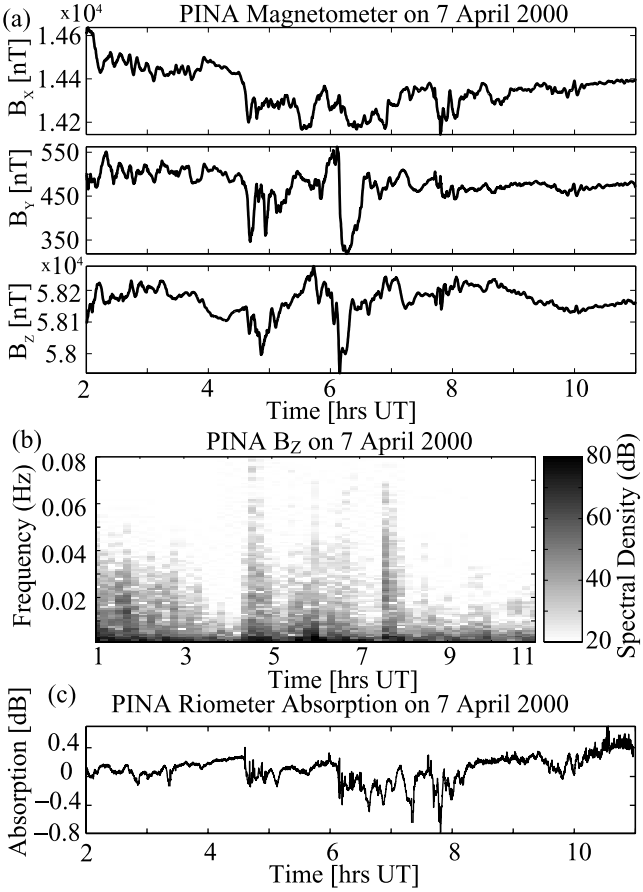

Figure 13. Magnetometer and riometer data from the CANOPUS array for 7 April 2000. The fluxgate magnetometer and riometer (PINA) was located in Pinawa in south central Canada (50.20°N, 96.04°W), north of the HAIL array at an *L* shell of 4.11 (see the PINA demarcation in Figure 3). (a) Magnetic field strength from 02:00 to 11:00 UT with measurement resolution of 0.025 nT and time resolution of 0.2 Hz. (b) Spectrogram of the magnetic field strength (B_z) for 7 April. The spectral density intensity (as depicted by the shading) of each spectral component is plotted vertically as a function of frequency (modulation frequency of the vertical magnetic field strength) and horizontally as a function of universal time. The spectrogram content represents the frequency content of the variations in the magnetic field strength measured at the PINA magnetometer. A pronounced increase in spectral content, extending up to ~0.05 Hz, can be seen starting at ~04:30 UT. The frequency content and timing of the magnetic field perturbations are similar to the VLF perturbations observed on 7 April 2000 (Figure 11). (c) Widebeam riometer (30 MHz) observations for 7 April 2000, with quiet day baseline subtracted. Absorption is positive for negative deflections.

quasiperiodic VLF signal amplitude fluctuations of the type considered in this paper, instead only considering isolated cases of amplitude and phase changes. However, some of the cases reported show similar signatures as reported here [i.e., *Cummer et al.*, 1996, Figures 7 and 9]. Given that the VLF perturbations (both the depression and subsequent fluctuations) observed in this paper coincided with the expansion of the equatorward edge of the auroral oval over the disturbed GCPs, we suggest that the signal perturbations are most likely a result of variations in high-energy auroral precipitation associated with the movement of the auroral electrojet.

4.2. "Zigzag Effect" and Pulsating Aurora

[33] *Carpenter et al.* [1997] reported on a type of signal variation called the "zigzag effect," which appeared on VLF/LF propagation paths in the $L = 4-5$ range and were characterized by quasi-periodic fluctuations with periods usually in the $\sim$5–60 s range but sometimes reaching $\sim$100 s. The "zigzag effect" has predominantly been observed at higher latitudes than those examined here, including stations at Siple, Antarctica ($L \sim 4.3$), Saskatoon, Canada ($L \sim 4.2$) [*Carpenter et al.*, 1997], and Kerguelen, Antarctica ($L \sim 3.7$) [*Corcuff*, 1996]. The horizontal extent of the perturbation region was inferred to have been in the range of $\sim$50–200 km, with the perturbation centered within $\sim$100–200 km of the affected signal paths.

[34] The fluctuations reported in the present paper are of a lower-frequency range with a broader frequency spectrum than the "zigzag effects" previously reported [*Carpenter et al.*, 1997], which had a periodicity in the $\sim$5–60 s range and sometimes exhibited a single discrete frequency of modulation. However, the fluctuations considered herein occur at lower latitudes and under more geomagnetically disturbed conditions than the previous observations of the "zigzag effect."

[35] Although predominantly a postmidnight phenomenon, VLF "zigzag" activity prior to local midnight has been observed at times of severe magnetic disturbance [*Carpenter et al.*, 1997]. *Carpenter et al.* [1997] reported that the "zigzag effect" was not observed during geomagnetically quiet conditions and exhibited earlier onsets with longer multihour durations when K_p was 5 or greater. The fluctuations in VLF amplitude signals observed on 7 April 2000 and 31 October 2003 began prior to local midnight and were of longer duration than previous observations of the "zigzag effect." Given the high geomagnetic activity during the nights of 7 April 2000 and 31 October 2003, the premidnight onset and long duration of the observed fluctuations are not inconsistent with previous observations of the "zigzag effect," although it is unclear whether the fluctuations observed here and the previous observations of zigzag activity are generated by the same source.

[36] The suggested underlying cause of the "zigzag effect" was pulsating auroral precipitation, with the more energetic ($E > 40$ keV) electrons in the incident electron spectrum causing secondary ionization and subsequent decay at or below 85 km [*Carpenter et al.*, 1997]. Pulsating aurora are mainly found in the midnight to morning sector on the equatorward side of the auroral oval and consist of irregularly shaped patches which appear to switch on and off with a varying periodicity between 2 and 20 s [*Sandahl*, 1985; *Nemzek et al.*, 1995]. They are typically thought to be a result of variations in the intensity of precipitating electrons. The precipitation is induced by coherent wave-particle interaction between energetic electrons and chorus waves near the equator [*Johnstone*, 1983], with the modulation possibly imposed on the electron precipitation by a type of relaxation oscillator involving the VLF whistler mode wave producing instabilities in the equatorial region [*Davidson and Chiu*, 1991].

[37] The energy ranges typically associated with altering the reflection height of VLF signals via secondary ionization are significantly higher than those typically associated with auroral precipitation [*Lev-Tov et al.*, 1995]. However, pulsating aurora is known to have a substantially harder spectrum [e.g., *Brown et al.*, 1976] than typical auroral precipitation, with direct satellite observations of pulsating aurora spectra extending up to energies of $\sim$100 keV [*Evans et al.*, 1987]. Furthermore, the electron precipitation fluxes in pulsating aurora are on average more intense, harder, and penetrate to lower latitudes as the level of geomagnetic activity increases [*Carpenter et al.*, 1997]. Given the intense nature of the geomagnetic storms examined in this paper, electron precipitation associated with pulsating aurora may have been energetic enough to contribute to the perturbations in VLF signal amplitude observed. Simultaneous measurements of VLF perturbations and ground based optical and/or satellite measurements of pulsating aurora during geomagnetic storms would be useful in determining the role of pulsating aurora in disturbing the *D* region ionosphere.

5. Conclusion

[38] We have examined the effects of two geomagnetic storms on the midlatitude *D* region using several VLF signal paths in both the northern and southern hemispheres. The amplitude and phase of the VLF signals exhibit perturbations with increased geomagnetic activity, with fluctuations in amplitude persisting several hours after the advent of the geomagnetic storm. We examined the frequency content of these fluctuations, as well as the location and timing of the disturbance, using multiple VLF signal paths and auroral activity patterns based on auroral flux measurements obtained by the NOAA-POES satellites. The depression and variation of the VLF signal amplitude are shown to be consistent with measured variations in the energetic electron precipitation flux as recorded by the NOAA-POES satellite.

[39] This paper demonstrates that subionospheric VLF signals can be used as a diagnostic of high-energy auroral precipitation at midlatitudes during disturbed geomagnetic conditions. The onset of fluctuations in the VLF amplitude data on 7 April 2000 occurred immediately after the depression of the signal amplitude, when auroral precipitation extended equatorward over the GCPs. The ability to locate and characterize the extension of auroral precipitation to lower latitudes can increase our understanding of the mechanisms and ionospheric effects of these massive geomagnetic storms.

[40] **Acknowledgments.** This work was supported by the National Science Foundation and the Office of Naval Research under grants ATM-9910532, OPP-0233955, and N00014-03-1-0333. We thank Dave Evans of NOAA for the use of NOAA-POES data and Don Carpenter for his useful

commentary. The authors thank the CARISMA team for provision of magnetometer data and thank E. Donovan and Emma Spanswick for provision of riometer data. CARISMA magnetometer and NORSTAR riometer data were provided through the Canadian Space Science Data Portal (SSDP). Operation of CARISMA, NORSTAR, and the SSDP is funded by the Canadian Space Agency. The authors thank I.R. Mann for useful discussions and comments on the manuscript.

[41] Arthur Richmond thanks Steven Cummer and another reviewer for their assistance in evaluating this paper.

References

Baker, D. N., S. G. Kanekal, X. Li, S. P. Monk, J. Goldstein, and J. L. Burch (2004), An extreme distortion of the Van Allen belt arising from the 'Hallowe'en' solar storm in 2003, *Nature*, *432*(7019), 878.

Brown, N. B., T. N. Davis, T. J. Hallinan, and G. C. Stenbaeck-Nielsen (1976), Altitude of pulsating aurora determined by a new instrumental technique, *Geophys. Res. Lett.*, *3*, 403.

Carpenter, D. L., and R. R. Anderson (1992), An ISEE/whistler model of equatorial electron density in the magnetosphere, *J. Geophys. Res.*, *97*, 1097.

Carpenter, D. L., M. Galand, T. F. Bell, V. S. Sonwalkar, U. S. Inan, J. LaBelle, A. J. Smith, T. D. G. Clark, and T. J. Rosenberg (1997), Quasiperiodic 5–60 s fluctuations of VLF signals propagating in the earth-ionosphere waveguide: A result of pulsating auroral particle precipitation?, *J. Geophys. Res.*, *102*, 347.

Chenette, D. L., D. W. Datlowe, R. M. Robinson, T. L. Schumaker, R. R. Vondrak, and J. D. Winningham (1993), Atmospheric energy input and ionization by energetic electrons during the geomagnetic storm of 8–9 November 1991, *Geophys. Res. Lett.*, *20*, 1323.

Corcuff, Y. (1996), Trimpi events and other amplitude perturbations observed during 1991 at Kerguelen (L = 3.7) on the subionospheric NWC signal, *J. Atmos. Terr. Phys.*, *58*, 1367.

Cummer, S. A., T. F. Bell, U. S. Inan, and L. J. Zanetti (1996), VLF remote sensing of the auroral electrojet, *J. Geophys. Res.*, *101*, 5381.

Cummer, S. A., T. F. Bell, and U. S. Inan (1997), VLF remote sensing of high-energy auroral particle precipitation, *J. Geophys. Res.*, *102*, 7477.

Davidson, G. T., and Y. T. Chiu (1991), An unusual nonlinear system in the magnetosphere: A possible driver for auroral pulsations, *J. Geophys. Res.*, *96*, 19,353.

Demirkol, M. K., U. S. Inan, T. F. Bell, S. G. Kanekal, and D. C. Wilkinson (1999), Ionospheric effects of relativistic electron enhancement events, *Geophys. Res. Lett.*, *26*, 3557.

Evans, D. S., G. T. Davidson, H. D. Voss, W. L. Imhof, J. Mobilia, and Y. T. Chiu (1987), Interpretation of electron spectra in morningside pulsating aurorae, *J. Geophys. Res.*, *92*, 12,295.

Ferguson, J. A., and F. P. Snyder (1987), The segmented waveguide programs for long wavelength propagation calculations, *Tech. Doc. 1071*, Naval Ocean Syst. Cent., San Diego, Calif.

Foster, J. C., S. Cummer, and U. S. Inan (1998), Midlatitude particle and electric field effects at the onset of the November 1993 geomagnetic storm, *J. Geophys. Res.*, *103*, 26,359.

Gaines, E. E., D. L. Chenette, W. L. Imhof, C. H. Jackman, and J. D. Winningham (1995), Relativistic electron fluxes in May 1992 and their effect on the middle atmosphere, *J. Geophys. Res.*, *100*, 1027.

Glukhov, V. S., V. P. Pasko, and U. S. Inan (1992), Relaxation of transient lower ionospheric disturbances caused by lightning-whistler-induced electron precipitation bursts, *J. Geophys. Res.*, *97*, 16,971.

Inan, U. S., and D. L. Carpenter (1987), Lightning-induced electron precipitation events observed at $L \sim 2.4$ as phase and amplitude perturbations on subionospheric VLF signals, *J. Geophys. Res.*, *92*, 3293.

Inan, U. S., D. L. Carpenter, R. A. Helliwell, and J. P. Katsufrakis (1985), Subionospheric VLF/LF phase perturbations produced by lightning-whistler induced particle precipitation, *J. Geophys. Res.*, *90*, 7457.

Johnstone, A. D. (1983), The mechanism of pulsating aurora, *Ann. Geophys.*, *1*, 397.

Kikuchi, T., and D. S. Evans (1983), Quantitative study of substorm-associated VLF phase anomalies and precipitating energetic electrons on November 13, 1979, *J. Geophys. Res.*, *88*, 871.

Lehtinen, N. G., U. S. Inan, and T. F. Bell (2001), Effects of thunderstorm-driven runaway electrons in the conjugate hemisphere: Purple sprites, ionization enhancements, and gamma rays, *J. Geophys. Res.*, *106*, 28,841.

Lev-Tov, S. J., U. S. Inan, and T. F. Bell (1995), Altitude profiles of localized D-region density disturbances produced in lightning-induced electron precipitation events, *J. Geophys. Res.*, *100*, 21,375.

Luo, M., S. Pullen, D. Akos, G. Xie, S. Datta-Barua, T. Walter, and P. Enge (2002), Assessment of ionospheric impact on LAAS using WAAS Supertruth data, paper presented at 58th Annual Meeting, Inst. of Nav., Albuquerque, N. M.

McEwen, D. J., C. N. Duncan, and R. Montalbetti (1981), Auroral electron energies: Comparisons of in situ measurements with spectroscopically inferred energies, *Can. J. Phys.*, *59*, 1116.

Nemzek, R. J., R. Nakamura, D. N. Baker, R. D. Belian, D. J. McComas, M. F. Thomsen, and T. Yamamoto (1995), The relationship between pulsating auroras observed from the ground and energetic electrons and plasma density measured at geosynchronous orbit, *J. Geophys. Res.*, *100*, 23,935.

Ostgaard, N., J. Stadsnes, J. Bjordal, G. A. Germany, R. R. Vondrak, G. K. Parks, S. A. Cummer, D. L. Chenette, and J. G. Pronko (2001), Auroral electron distributions derived from combined UV and X-ray emissions, *J. Geophys. Res.*, *106*, 26,081.

Pasko, V. P., and U. S. Inan (1994), Recovery signatures of lightning-associated VLF perturbations as a measure of the lower ionosphere, *J. Geophys. Res.*, *99*, 17,523.

Peter, W. B., and U. S. Inan (2004), On the occurrence and spatial extent of electron precipitation induced by oblique nonducted whistler waves, *J. Geophys. Res.*, *109*, A12215, doi:10.1029/2004JA010412.

Poulsen, W. L., U. S. Inan, and T. F. Bell (1993), A multiple-mode three-dimensional model of VLF propagation in the earth-ionosphere waveguide in the presence of localized *D* region disturbances, *J. Geophys. Res.*, *98*, 1705.

Rees, M. H., D. Lummerzheim, R. G. Roble, J. D. Winningham, J. D. Craven, and L. A. Frank (1988), Auroral energy deposition rate, characteristic electron energy, and ionospheric parameters derived from dynamics explorer 1 images, *J. Geophys. Res.*, *93*, 12,841.

Ringlee, R. J. (1989), Geomagnetic effects on power systems, *IEEE Power Eng. Rev.*, *9*, 6.

Sandahl, I. (1985), Recent developments in pulsating aurora studies, paper presented at the 13th Annual Meeting on Upper Atmosphere Studies by Optical Methods, Kiruna Geophys. Inst., Oslo, Norway.

Smith, A. J., M. J. Engebretson, E. M. Klatt, U. S. Inan, R. L. Arnoldy, and H. Fukunishi (1998), Periodic and quasiperiodic ELF/VLF emissions observed by an array of Antarctic stations, *J. Geophys. Res.*, *103*, 23,611.

Smith, A. J., M. P. Freeman, S. Hunter, and D. K. Milling (2002), VLF, magnetic bay, and Pi2 substorm signatures at auroral and midlatitude ground stations, *J. Geophys. Res.*, *107*(A12), 1439, doi:10.1029/2002JA009389.

Stauning, P. (1997), Substorm modeling based on observations of an intense high-latitude absorption surge event, *J. Geophys. Res.*, *103*, 26,433.

Uberall, H., A. Nagl, and J. B. Seaborn (1982), Coupled-mode propagation in the ionospheric day-night transition region, *Radio Sci.*, *17*, 870.

Wolf, T. G., and U. S. Inan (1990), Path-dependent properties of subionospheric VLF amplitude and phase perturbations associated with lightning, *J. Geophys. Res.*, *95*, 20,997.

Wood, T. G., and U. S. Inan (2002), Long-range tracking of thunderstorms using sferic measurements, *J. Geophys. Res.*, *107*(D21), 4553, doi:10.1029/2001JD002008.

M. W. Chevalier, U. S. Inan, and W. B. Peter, STAR Laboratory, Stanford University, 351 Packard Bldg., Stanford, CA 94305, USA. (wpeter@stanford.edu)